Asian Journal of Water, Environment and Pollution, Vol. 13, No. 3 (2016), pp. 15–27.
DOI 10.3233/AJW-160023

Analysis of Spatially and Temporally Varying Precipitation in Bangladesh

Ahmad Hasan Nury*, Khairul Hasan, Kazi Mohammed Erfan and Debashis Chandra Dey

Civil & Environmental Engineering, Shahjalal University of Science & Technology, Sylhet, Bangladesh
✉ hasancee10@gmail.com

Received March 1, 2016; revised and accepted June 21, 2016

Abstract: Nowadays, time series analysis of rainfall data is a major tool to explore rainfall variability pattern. In this study, rainfall data at 28 stations of Bangladesh has been evaluated using trend test, spatial analysis and Artificial Neural Network (ANN) model. From the Mann-Kendall's (M-K) trend test, it was observed that the value of Sen's slope for the maximum increase of rainfall was 1.813 mm per month in Cox's Bazar and the maximum decrease of rainfall was -0.896 mm per month in Bhola. Rainfall time series were smoothed using wavelet transformation and then wavelet denoised signals were used for fitting Artificial Neural Network (ANN) model. The predictive capability of ANN model was assessed by PBIAS (Percent of bias), index of agreement (*d*) and *R*-squared approach. Finally, a forecast for five years (January 2010-December 2014) was carried out to evaluate the predictive capability. The values of normalized root mean square error (NRMSE) ranges between 0.07% and 0.17% for calibration and 0.07%-0.32% for validation which indicate the fitness of the model. The findings derived from the study are to understand the nature of possible rainfall variations in 28 stations of Bangladesh, which will help the hydrologists as well as the policy makers to make decisions.

Key words: Autocorrelation, Mann-Kendall test, spatial distribution, ANN, wavelet-ANN.

Introduction

Variations in rainfall are one of the most critical factors determining the overall impact of climate change. According to the Fourth Assessment Report of Intergovernmental Panel on Climate Change (IPCC) (IPCC, 2007), it was observed that for most of the North America and especially over high-latitude areas in Canada, annual rainfall has increased during the 105-years period. Rainfall trends have considerable effects on environment and human resources. One of the vital aspects of climate change is the variation in rainfall. Food production is mostly sensitive to the rainfall variation, because crop harvesting directly depends on climatic circumstances like rainfall patterns. High rainfall will lead to large declines in cereal (e.g. rice, wheat) production around the world (Stern, 2007). In Chittagong city, landslide phenomena is the major concerning issue which causes countless problems to the life and properties and it is increasing day by day. At least ten landslide events happened during 2000-2009, where rainfall was a prompting factor in most scenarios (Khan et al., 2011). Heavy rainfall is responsible for putting many communities at risk for devastation from floods. Flooding can cause a variety of health hazards and risks, including death and injury, spilling of hazardous material, contaminated drinking water, increased population of disease-carrying insects and rodents, moldy houses, and community disruption and

*Corresponding Author

displacement. Flood also carries an enormous quantity of sediment to the rivers and streams.

The non-parametric Mann-Kendall (M–K) test can be used to detect trends in time-series analysis (Longobardi et al., 2009; Miao et al., 2012; Modarres and Sarhadi, 2009; Nasri and Modarres, 2009; Ramazanipour and Roshani, 2011; Shamsuddin, 2011; Partal and Kahya, 2005; Yue et al., 2002). Miao et al. (2012) represented that the rank based non-parametric MK trend test was frequently used to measure the significance of trends in time series data. The study had done a widespread revise on trend and periodicity of the seasonal data for the period of 1724-2009 in Beijing, China. For studying the trend in rainfall, linear regression analysis and non-parametric MK test were applied.

Spatial distribution using multiple linear regression and Geographic Information System (GIS) techniques can be used for analyzing the rainfall variation (Luís et al., 2000; Marquínez et al., 2003; Cannarozzo et al., 2006; Hand and Shepherd, 2009; Shamsuddin, 2007; Shahid and Khairulmaini, 2009). Shahid and Khairulmaini (2009) worked on spatial and temporal variability of rainfall in Bangladesh. This study was conducted over a time period of thirty-five years (1969-2003) and rainfall data was collected from 24 rain gauge stations over the country. Using kriging method long-term annual average rainfall, coefficient of variation of annual rainfall, rainfall concentration and aridity indices at each station were calculated and then interpolated within a geographic information system to illustrate the temporal and spatial variability of rainfall.

Wavelet transformation decomposes the original time series into subcomponents so that the decomposed data develop the performance of geophysical and hydrological prediction models by capturing useful information at various resolution levels. Recently, the combined wavelet-artificial neural network (Wavelet-ANN) model has been widely used to forecast hydrological and hydrogeological phenomena (Agarwal et al., 2012; Akhtar et al., 2009; Alrumiah and Fawzan, 2002; Nakhei and Nasr, 2012; Nejad and Nourani, 2012; KİSİ, 2003; Panigrahi et al., 2013; Pinto et al., 2012). Nakhaei and Nasr (2012) developed Wavelet-Artificial Neural Network (WANN) model, using discrete wavelet transform method and different mother wavelets (Haar, db2, db3 and db4) to decompose groundwater level time series into sub-signals and reconstruct the forecast time series of six months ahead using ANN model.

The present study aims at analyzing the trend and pattern of rainfall of the 28 stations of Bangladesh to see the transient variations. Here, seasonal MK trend test was applied. It also develops a method using wavelet technique to predict monthly rainfall.

Study Area and Data Collection

Bangladesh, on the northern coast of the Bay of Bengal, is surrounded by India, with a small common border with Myanmar in the South-East, located at 23.70° N latitude and 90.35° E longitude. The country is low-lying riverine land crossed by the many branches and tributaries of the Ganges and Brahmaputra rivers. In addition, Bangladesh has a tropical monsoon climate which consists of heavy seasonal rainfall, high temperatures and high humidity. Natural disasters such as floods, tornadoes, and tidal bores affect the country yearly. The rainfall season of Bangladesh can be categorized into four seasons such as pre-monsoon (March-May), monsoon (June-September), post-monsoon (October-November) and winter (December-February). Most rains occur during the monsoon (June-September) and little in winter (December-February).

The climate of Bangladesh is categorized into seven climatic sub-regions such as South-Eastern zone, North-Eastern zone, Northern part of the Northern region, North-Western zone, Western zone, South-Western zone and South-central zone. However, rainfall stations were selected cautiously so that they represent all the sub regions properly. Table 1 represents the climatic sub-regions of Bangladesh.

Table 1: Climatic sub-regions of Bangladesh

Zone	*Climatic sub-regions*	*Stations*
A	South-Eastern zone	Bhola, Barisal, Chi (Patenga), Cox's Bazar, Feni, Hatia, Khepupara, Maijdi Court, Patuakhali, Rangamati, Sandwip, Sitakunda, Teknaf
B	North-Eastern zone	Sylhet, Srimongal
C	Northern part of the Northern region	Rangpur
D	North-Western zone	Bogra, Dinajpur, Ishurdi
E	Western zone	Rajshahi
F	South-Western zone	Jessore, Khulna, Satkhira
G	South-central zone	Comilla, Chandpur, Dhaka, Faridpur, Mymensingh

Monthly rainfall data of Barisal, Bhola, Bogra, Chandpur, Chi (Patenga), Comilla, Cox's Bazar, Dhaka, Dinajpur, Faridpur, Feni, Hatia, Ishurdi, Jessore, Khepupara, Khulna, Maijdi Court, Mymensingh, Patuakhali, Rajshahi, Rangamati, Rangpur, Sandwip, Satkhira, Sitakunda, Srimongal, Sylhet and Teknaf (28 stations) of Bangladesh have been collected from the Bangladesh Meteorological Department (BMD), which is the authorized Government organization for meteorological activities of Bangladesh. Figure 1 shows a map with the locations of the rainfall stations that were used.

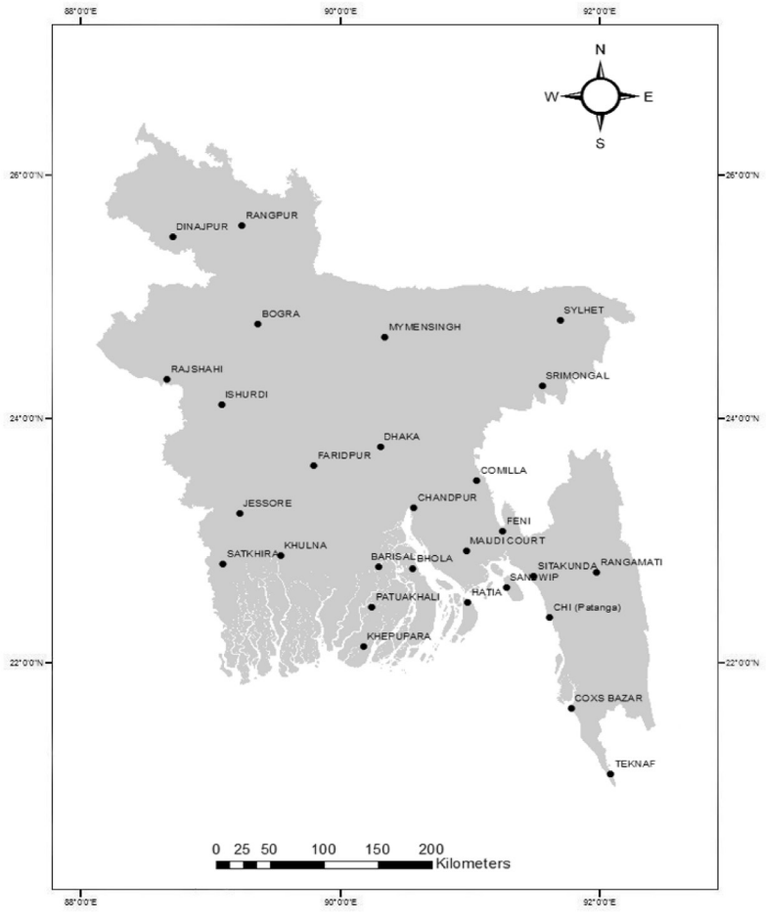

Figure 1: Locations of rainfall stations.

Methods

Trend Analysis

There are two types of trend analysis methods; parametric methods and non-parametric methods. Non-parametric tests are more suitable than their parametric counterparts when the data do not meet the assumption of normality (Afzal et al., 2011). In hydrologic and climatologic time series non-parametric MK trend test is widely used as a statistical test (Yue and Wang, 2004).

Mann-Kendall (M-K) test is a two-tailed test. It considers the time series of n data points and y_i and y_j as two subsets of data, where $i = 1, 2, 3, 4, \ldots, n-1$ and $j = i+1, i+2, i+3, i+4, \ldots, n$. The final value of S can be computed from the net result of all such increased and decreased values (Drápela and Drápelová, 2011).

The test statistic, S (Score) is computed as

$$S = \sum_{i=1}^{n-1} \sum_{j=i+1}^{n} \sin\,(y_j - y_i) \qquad (1)$$

$$\text{where } \sin\,(y_j - y_i) = \begin{cases} 1 \text{ if } y_j - y_i > 0 \\ 0 \text{ if } y_j - y_i = 0 \\ -1 \text{ if } y_j - y_i < 0 \end{cases} \qquad (2)$$

where y_j and y_i are the annual values in years j and i, $j > i$ respectively.

For determining the magnitude of trend in hydrological time series Sen's estimator has been used widely. Sen's method uses a linear model to estimate the slope of the trend (Salmi et al., 2002).

In Seasonal Mann-Kendall test, depending on the nature of the time series, a season could be a month or a quarter of a year, a year or any combination of these. So for monthly "seasons", January data are compared only with January, February only with February, etc., so that, overall, there are m = 12 seasons. No comparisons are made across season boundaries (Nury and Hasan, 2015).

Here, S' is the sum of Kendall's S, computed as discussed in the previous section for each season g.

$$S' = \sum_{g=1}^{m} S_g \tag{3}$$

In the parametric method, a scatter plot of the dependent variable and the independent variable is constructed. A least-squares linear regression line is then superimposed on the plot.

Spatial Distribution

A geographical information system (GIS) is introduced as a suitable tool for mapping the spatial distribution of rainfall and Sen's slope. Five maps are generated based on Sen's slope and total rainfall of each decade.

Geostatistical Analyst is innovative because it links the gap between geostatistics and GIS. Integration is essential because GIS can quantify the quality of the surface models by assessing the statistical error of predicted surfaces.

In interpolation technique the adjacent measured values are weighted to develop a predicted value for an unmeasured location. Weights are based on the distance between the measured points, the prediction locations, and the overall spatial preparation among the measured points.

The ordinary kriging model is expressed as:

$$Z(s) = \mu + \varepsilon(s) \tag{4}$$

where $\boldsymbol{s} = (X, Y)$ is a location and $Z(\boldsymbol{s})$ is the value at that location.

Wavelet Analysis

Nowadays wavelet analysis has become a popular tool due to its ability to expose information within the signal in both the time and scale (frequency) domains. General characteristics of wavelets are: they have wavelet oscillation with amplitude which begins at zero, increases and finally decreases back to zero. It is a mathematical model which transforms the original signal into a different domain for analysis and processing (Dong et al., 2001). We applied wavelet transform because it is very suitable with the non-stationary data. Climatic time series data as well as financial time series data are non-stationary (Wadi et al., 2011).

At first Morlet declared wavelets as a family of functions generated from translations and dilations of a single function which is known as the "mother wavelet". They can be computed by:

$$\Psi_{a,b}(t) = \frac{1}{\sqrt{|a|}} \Psi\left(\frac{t-b}{a}\right); a, b \varepsilon R; a \neq 0 \tag{5}$$

where 'a' is referred as scaling parameter or scale which measures the degree of compression. 'b' is referred as translation parameter which measures the time location of the wavelet. When $|a| < 1$ it means that the wavelet in (a) the compressed mother wavelet and corresponds to higher frequencies. On the contrary, when $|a| > 1$ it means that $\Psi_{a,b}(t)$ has a larger time-width than $\Psi(t)$ and corresponds to lower frequencies. This is why in signal processing and time-frequency signal analysis Morlet wavelets are most successful.

In wavelet transforms time domain is considered as the original domain. It transforms the time domain to time scale domain. By these processes the original time domain signal can be recovered without losing any information. Wavelet transforms also has a reverse process which is known as signal reconstruction or inverse wavelet transform (Yu et al., 2000).

Coupled Wavelet and ANN (Wavelet-ANN) Model

An Artificial Neural Network (ANN) is a data processing model that is motivated by the biological nervous systems such as the brain, process information. The application of ANNs to hydrological problems is promptly attaining acceptance due to their enormous power and potential in the mapping of nonlinear system data (KİSİ, 2003).

A set of inputs and outputs is designated from the training set and the network computes the output based on the inputs in the back-propagation algorithm (KİSİ, 2003). When the training is complete, the ANN performance is validated. Either the ANN has to be retrained or it can be applied for its projected use depending on the outcome. The more the input data, the better performance of the ANN. The number of the input, output and hidden layer nodes depend upon

the original data series. The network may occasionally over fit the data and the training may take a long time if the number of nodes in the hidden layer is too high (Agarwal et al., 2012).

The Levenberg–Marquardt (LM) algorithm was utilized to train the ANN models because it has been shown to be fast, accurate, and reliable (Adamowski and Karapataki, 2010).

Predictive Capability of ANN Model

The perfection of a forecast model is mainly dependent on its accuracy, how closely the model forecasts the actual result. The most important and useful predictive capability are root mean square error (RMSE), percent of Bias (PBIAS) and index of agreement (*d*) (Nury et al., 2015). Root mean square error is an estimate of the standard deviation of the random components in the data, and the best model has a minimum RMSE. The percent of bias measures the average tendency of the simulated data to be larger or smaller than the observed counterparts. The optimal PBIAS value is 0.0, and low values indicate accurate model simulations. The index of agreement measures the degree of model forecast error and varies from 0 (no correlation) to 1 (perfect fit).

$$\text{RMSE} = \sqrt{\sum_{t=1}^{n} \frac{\left[y_t(obs) - y_t(pred)\right]^2}{n}} \quad (6)$$

$$\text{PBIAS}(\%) = \frac{\sum_{i=1}^{N}(O_i - P_i) - 100}{\sum_{i=1}^{N} O_i} \quad (7)$$

$$d = 1.0 - \frac{\sum_{i=1}^{N}|O_i - P_i|}{\sum_{i=1}^{N}\left(|P_i - \bar{O}| + |O_i - \bar{O}|\right)} \quad (8)$$

where O_i, P_i and $\bar{O}$ are the observed data, the model-simulated data and the observed mean, respectively.

Results and Discussion

The variation of rainfall within last 40 years of time period was conducted by rainfall-decade bar diagram. Figure 2 shows the rainfall-decade bar diagram of Barisal station where rainfall is decreasing and Figure 3 illustrates the rainfall-decade bar diagram of Teknaf station where rainfall is increasing. Figure 4 represents the spatial distribution of total rainfall of four decades of all 28 stations. Among all the four decades the lowest

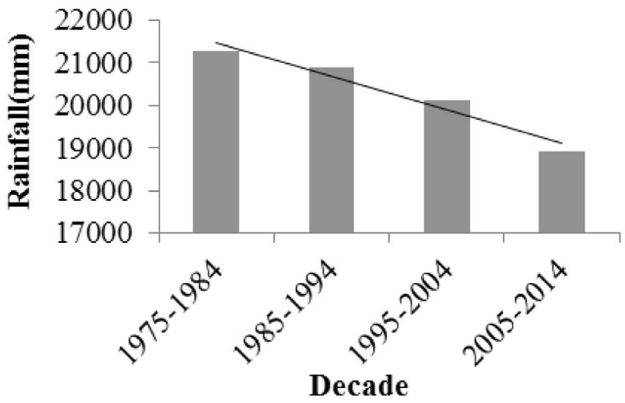

Figure 2: Rainfall-decade bar diagram of Barisal.

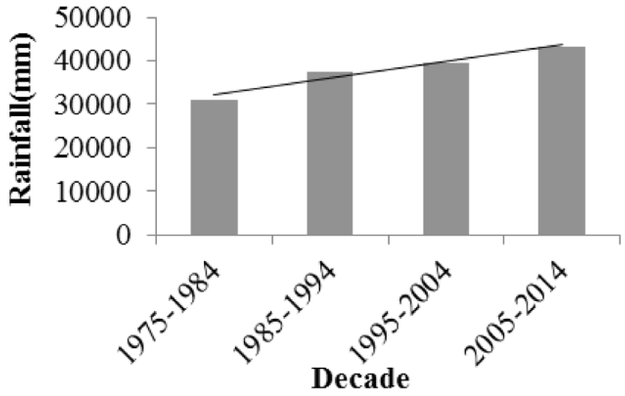

Figure 3: Rainfall-decade bar diagram of Teknaf.

amount of rainfall is found 12433 mm at Rajshahi and the highest amount of rainfall is found 43230 mm at Teknaf.

Trends of monthly rainfall have been conducted for each of the selected stations by linear regression analysis. The summary of the trend test is presented in Table 2.

A positive value of % of fluctuations rate (mm) refers to an increasing trend whereas a negative value refers to a decreasing trend. Figure 5 represents the higher increasing rate which is 0.92 mm per hundred years at Teknaf and Figure 6 denotes the higher decreasing rate which is 0.36 mm per hundred years at Bhola. Shahid and Khairulmaini (2009) also found that annual rainfall trend of Teknaf shows highest positive change of rainfall whereas Bhola shows the highest negative change of rainfall.

Autocorrelation check was conducted for finding the seasonality in the time series. Figure 7 shows that seasonality lies within the series of Dhaka station. Seasonality was also found for all other rainfall stations also. That's why seasonal MK test was used for detecting trend.

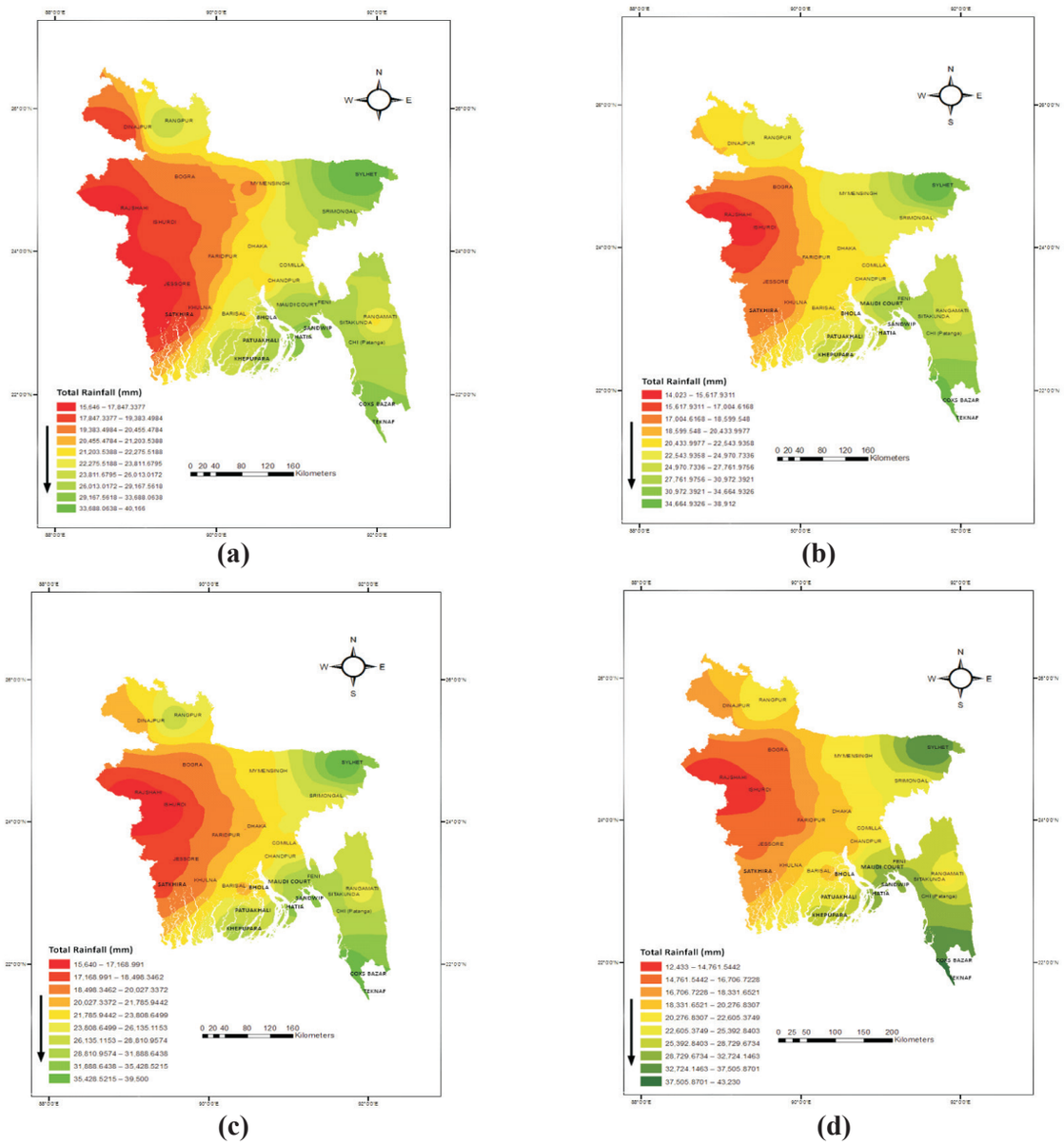

Figure 4: Spatial distribution of total rainfall of the four decades (a) 1975-84, (b) 1985-1994, (c) 1995-2004 and (d) 2005-2014.

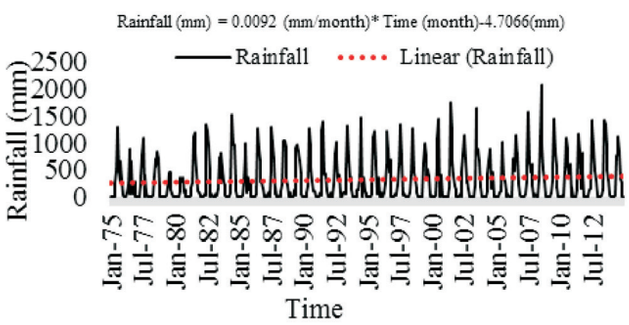

Figure 5: Linear trend for monthly rainfall (Teknaf).

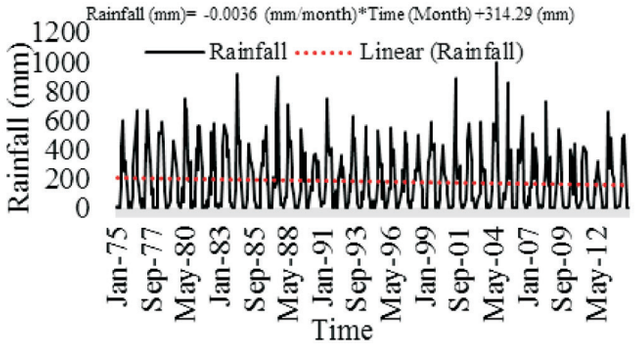

Figure 6: Linear trend for monthly rainfall (Bhola).

Table 2: Linear trends for monthly rainfall of selected stations

Station	*Rainfall*	
	% of fluctuations rate (mm)	*Climate line (mm)*
Barisal	-.16	223.22
Bhola	-.36	314.29
Bogra	-.22	224.33
Chandpur	.04	156.62
Chi(Patanga)	.27	145.93
Comilla	-.03	181.17
Cox`s Bazar	.47	125.79
Dhaka	-.21	243
Dinajpur	-.03	170.61
Faridpur	-.25	236.38
Feni	.11	202.64
Hatia	.19	190.12
Ishurdi	-.31	238.23
Jessore	.07	113.25
Khepupara	.17	169.49
Khulna	.04	136.46
Maijdi Court	.04	235.02
Mymensingh	.02	174.39
Patuakhali	.005	210.64
Rajshahi	-.18	182.08
Rangamati	-.06	206.89
Rangpur	-.11	249.28
Sandwip	.32	181.29
Satkhira	.04	130.36
Sitakunda	.19	180.99
Srimongal	-.14	248.62
Sylhet	-.10	361.29
Teknaf	.92	-4.7066

Mann-Kendall trend test depicts both positive and negative values of Sen's slope which are shown in Table 3. The maximum increase of rainfall which is 1.813 mm per month at Cox's Bazar and the maximum decrease of rainfall which is -0.896 mm per month at Bhola. Figure 8 shows in which stations trends were found, using ArcGIS. Trends were found in 17 stations out of 28 stations.

By using measured sample points of all the selected stations, geostatistical analyst tool (ArcGIS) is able to create an accurate predictions for other unmeasured points within the study area (ESRI, 2001). Figure 9

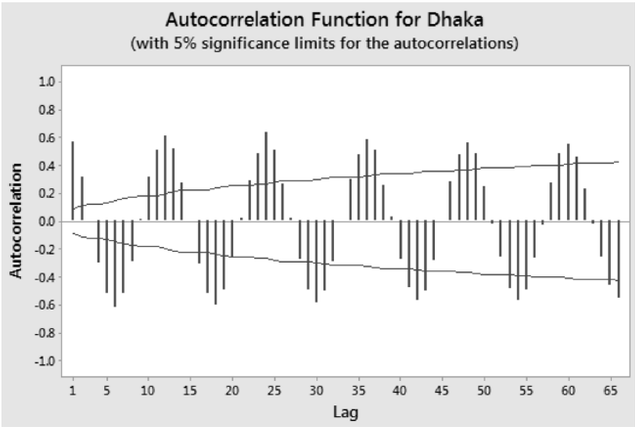

Figure 7: Autocorrelation check for monthly rainfall (Dhaka).

represents the spatial distribution of Sen's slope using ArcGIS. It represents that rainfall is high in the east and south-east region of Bangladesh. And rainfall is comparatively low in the north-east, north-west and south-west region.

Wavelet transformation decomposed the time series into time–frequency space, enabling the identification of both the dominant modes of variability and how those modes vary with time. For dealing with a very irregular data series, an irregular wavelet, the Daubechies wavelet of order 5 (DB5), has been used at level 3 (Ramna et al., 2013). Consequently, the detail time series are D1, D2, D3, and the approximation time series is A3 as shown in Figure 10 which shows the wavelet decomposition of rainfall signal at Feni respectively.

Table 4 shows the denoising results attained with various wavelet families for different noise structures such as unscaled white noise, scaled white noise and non-white noise of the rainfall. It is observed that the statistical parameter values of denoised signal using unscaled white noise gives better result as compared to scaled white noise and non-white noise structures and are less difference to original rainfall values. So unscaled white noise structure was used for denoising signal.

Figures 11 and 12 represent the original and denoised signal of rainfall at Feni station respectively. The outliers or noise are removed from the denoised signal, whereas the trend is same as original series and it is the main mechanism of wavelet denoising.

A rainfall data series may be multivariate and nonlinear, and the variables used may also have complex interrelationships (Ramna et al., 2013). MATLAB was used for model fitting by Artificial Neural Network (ANN) process. MATLAB solves

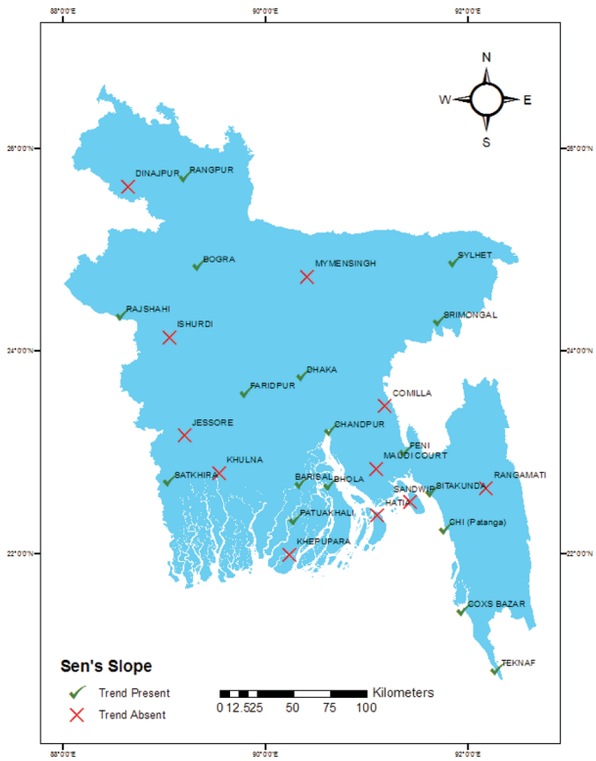

Figure 8: Spatial distribution of trend.

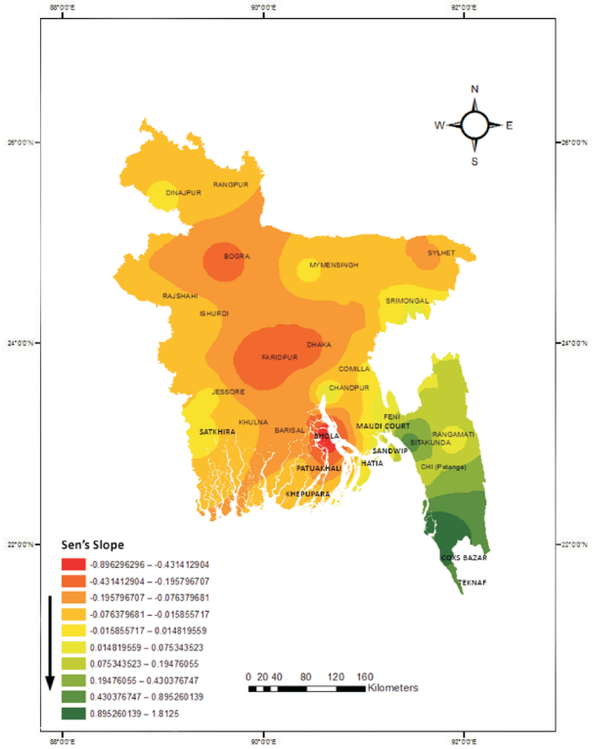

Figure 9: Spatial distribution of Sen's slope.

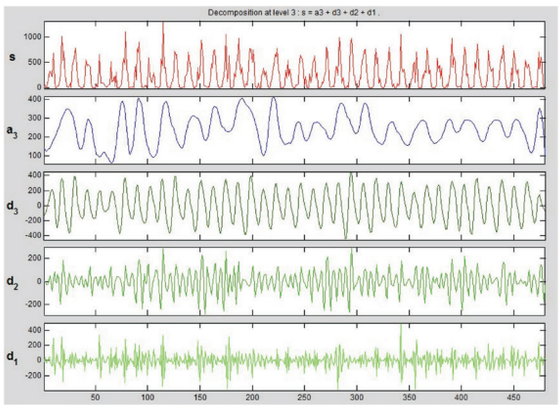

Figure 10: Wavelet decomposition of rainfall signal at Feni.

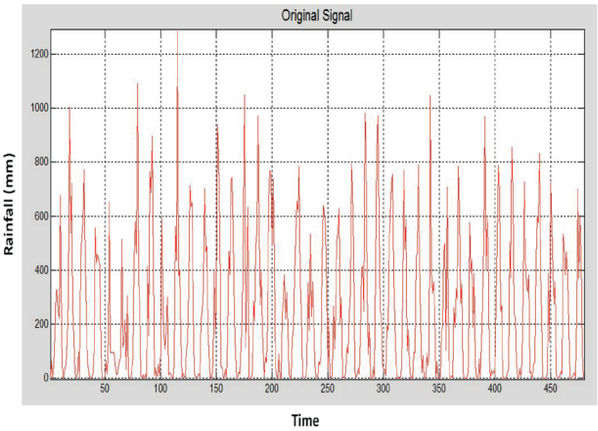

Figure 11: Wavelet original signal of rainfall at Feni.

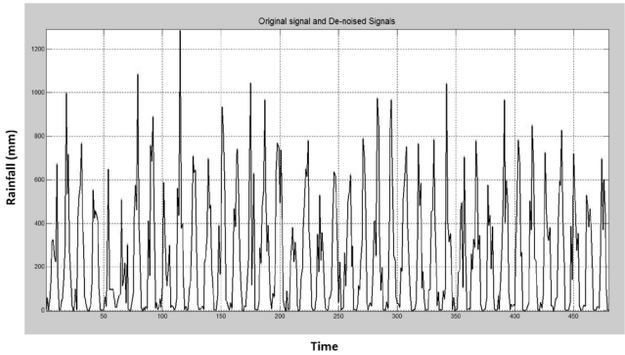

Figure 12: Wavelet denoised signal of rainfall at Feni.

Table 3: Mann-Kendall trend test for detecting trend of the selected stations

Station	*Sen's slope*	*Trend*
Barisal	-0.112	Yes
Bhola	-0.896	Yes
Bogra	-0.267	Yes
Chandpur	0.071	Yes
Chi(Patanga)	0.078	Yes
Comilla	0	No
Cox`s Bazar	1.813	Yes
Dhaka	-0.266	Yes
Dinajpur	0	No
Faridpur	-0.38	Yes
Feni	0.063	Yes
Hatia	0	No
Ishurdi	0	No
Jessore	0	No
Khepupara	0	No
Khulna	0	No
Maijdi Court	0	No
Mymensingh	0	No
Patuakhali	-0.025	Yes
Rajshahi	-0.062	Yes
Rangamati	0	No
Rangpur	-0.03	Yes
Sandwip	0	No
Satkhira	0.024	Yes
Sitakunda	0.667	Yes
Srimongal	0.017	Yes
Sylhet	-0.091	Yes
Teknaf	0.545	Yes

many technical computing problems with matrix and vector formulations, in a fraction of the time (Agrawal et al., 2012). The Levenberg-Marquardt (LM) algorithm was used to train the ANN models because it gives a better exchange between the stability of the steepest descent method and the speed of the Newton algorithm (Adamowski and Karapataki, 2010).

The data of denoised signal were used as target and the data from wavelet decomposition (approximations and details) were used as input. The data was randomly divided into three groups, 70% of the data corresponds to training group, 15% of the data corresponds to testing group and 15% corresponds to validation group (Alrumiah and Fawzan, 2002). January 2010 to December 2014 (five years) of data were predicted by using Artificial Neural Network.

Table 5 represents the performance of model fitting of all 28 stations. In network architecture no. of delays were 2 with one hidden layer (Ramana et al., 2013). A trial and error method was induced with one hidden layer for identifying the suitable number of hidden neurons. The number of hidden neurons was increased from 1 to 20 for finding the best fitted model (Ramana et al., 2013). *R*-squared is defined as a statistical measure of how close the data are fitted to the regression line (Alrumiah and Fawzan, 2010). The network train the data series within epoch 1 to 1000. Then index of agreement covers between 0.953295 and 0.999226 which means that the model is fitted properly (Deo and Shahin, 2015).

The adequacy of the fitted model were checked by using root mean square error (RMSE) and normalized root mean square error (NRMSE). The whole data set was divided into two parts namely calibration and validation (Ramana et al., 2013). For calculating the calibration, the data of 420 months (1975-2009) were used and for calculating the validation the data of 60 months (2010-2014) are used.

Table 4: Level 3 decomposition of rainfall signal using Daubechies5 wavelet

Statistical parameter	*Denoised signal*			
	Original rainfall	*Unscaled white noise*	*Scaled white noise*	*Non-white noise*
Mean	169.1854	169.1766	169.019	169.059
Standard deviation	177.6406	175.5872	86.15851	48.59367
Max	1025	1018.119	604.1663	454.9272
Min	0	-3.37829	-10.2702	48.77998
Range	1025	1021.497	614.4365	406.1472
Mean absolute deviation	146.6786	144.9646	70.27321	37.46004

Table 5: Network performance and predictive capability of ANN model

Stations	*Network architecture*	*R-squared*	*PBIAS*	*Index of agreement*	*Epoch no.*
Barisal	2-1-10	0.93447	0.64312	0.996787	5
Bhola	2-1-10	0.95746	1.0298	0.994812	9
Bogra	2-1-8	0.94383	1.2785	0.983293	3
Chandpur	2-1-10	0.94155	0.90595	0.99548	25
Chi(Patenga)	2-1-10	0.96777	0.67798	0.996613	6
Comilla	2-1-10	0.94912	1.878439	0.985362	9
Cox`s Bazar	2-1-10	0.96362	0.7037	0.996485	8
Dhaka	2-1-10	0.95252	1.99634	0.985205	7
Dinajpur	2-1-10	0.95155	1.52991	0.973032	6
Faridpur	2-1-10	0.94806	1.417038	0.992847	11
Feni	2-1-10	0.95861	0.9546	0.999226	10
Hatia	2-1-10	0.95531	1.15849	0.994227	7
Ishurdi	2-1-10	0.93305	0.902849	0.953295	3
Jessore	2-1-10	0.94118	1.29807	0.988613	7
Khepupara	2-1-10	0.951	1.38935	0.988166	6
Khulna	2-1-10	0.9376	1.35473	0.988057	7
Maijdi Court	2-1-10	0.93916	1.46803	0.982311	6
Mymensingh	2-1-10	0.94743	0.93074	0.958606	5
Patuakhali	2-1-10	0.97449	1.08229	0.994605	17
Rajshahi	2-1-10	0.96047	0.72025	0.996377	6
Rangamati	2-1-10	0.96219	1.44913	0.983007	10
Rangpur	2-1-10	0.95492	0.75409	0.991131	13
Sandwip	2-1-10	0.94238	1.29613	0.988623	9
Satkhira	2-1-10	0.95255	1.48685	0.982824	7
Sitakunda	2-1-10	0.95111	0.92896	0.998731	6
Srimongal	2-1-10	0.94199	0.93377	0.990213	9
Sylhet	2-1-10	0.9521	1.55859	0.997208	7
Teknaf	2-1-10	0.97995	2.390655	0.987873	15

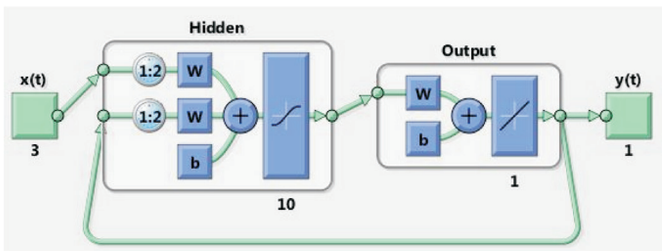

Figure 13: Neural network of Feni station.

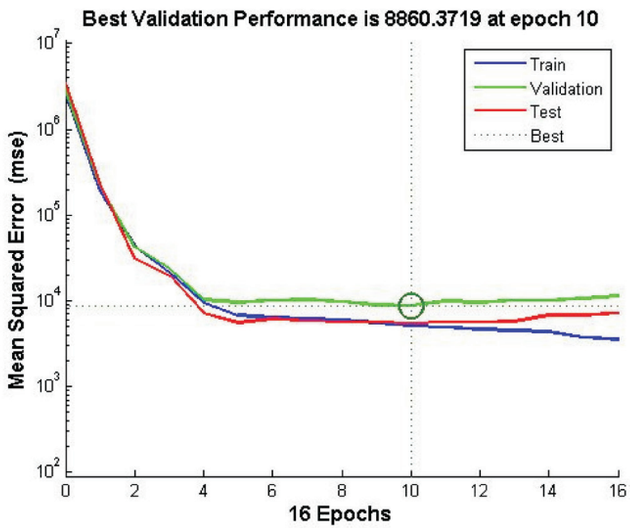

Figure 14: Neural network training performance of Feni.

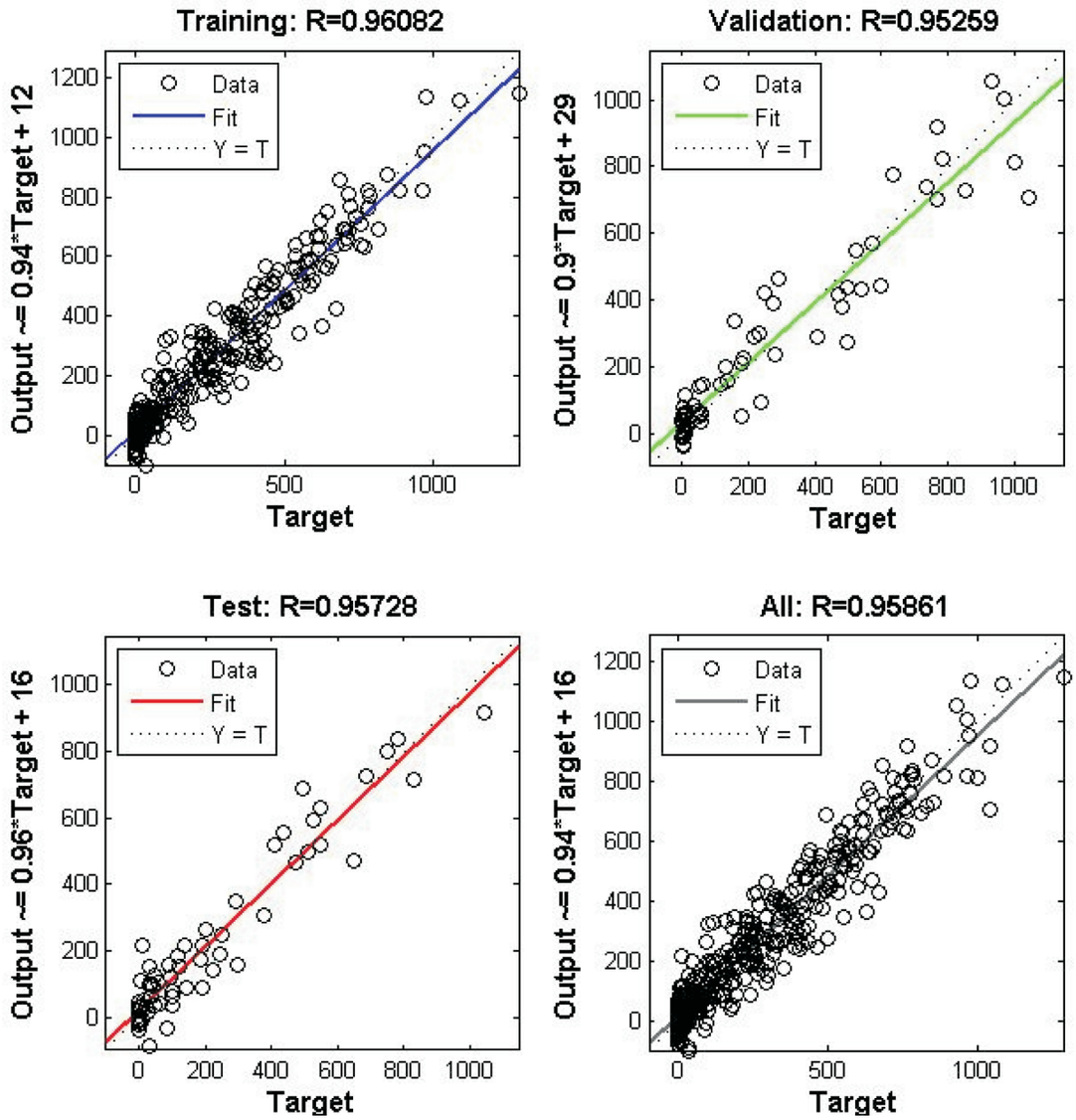

Figure 15: Regression analysis of neural network for Feni.

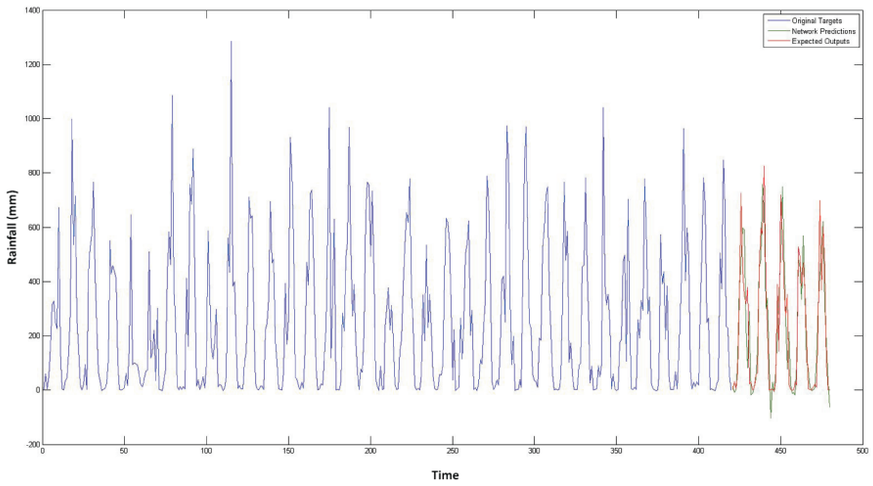

Figure 16: Rainfall predictions using neural network for Feni.

Figure 13 represents the number of hidden neurons for training the network of the Feni station and Figure 14 indicates the best validation performance at epoch 10. Figure 15 shows that the values of Regression (*R*) for training, validation and testing is near to 1 (> .9) which represents that the model is fitted well.

Figure 16 shows the prediction of rainfall for five years (January 2010- December 2014) of Feni. The blue line indicates the original target or rainfall data series, the red line indicates the expected outputs and the green line indicates the network predictions or rainfall predictions for five years. It is observed that the expected outputs and network predictions are almost same, it defines the accuracy of the predictions and model fitting.

Conclusion

A comprehensive assessment about the characteristics of rainfall and forecasting of rainfall at 28 stations of Bangladesh are represented in this study. Rainfall is decreasing in last 40 years at Barisal, Bhola, Bogra, Chandpur, Comilla, Dhaka, Dinajpur, Faridpur, Ishurdi, Mymensingh, Patuakhali, Rajshahi, Rangamati, Rangpur, Srimongal and Sylhet stations respectively. On the other hand, rainfall is increasing at Chittagong (Patenga), Cox's Bazar, Feni, Hatia, Jessore, Khepupara, Maijdi-Court, Rangamati, Sandwip, Satkhira, Sitakunda and Teknaf stations respectively. From the linear trend analysis it was observed that higher increasing trend was found 0.92 mm per hundred years at Teknaf and higher decreasing trend was found 0.36 mm per hundred years at Bhola. Seasonal MK test specifies that the value of Sen's slope for the maximum increase of rainfall was 1.813 mm per month at Cox's Bazar and the maximum decrease of rainfall was -0.896 mm per month at Bhola. From the trend test for Sen's slope it was observed that trends were found in 17 stations out of 28 stations using ArcGIS. From the spatial distribution of Sen's slope it was found that Cox's Bazar shows the highest positive change of rainfall whereas Bhola shows the highest negative change of rainfall. For prediction, the time series of rainfall were smoothed using wavelet transformation, then wavelet denoised signals were used for fitting ANN model. Finally ANN model was fitted using Levenberg-Marquardt (LM) algorithm based on *R*-squared. Finally, a forecast for five years (January 2010-December 2014) was carried out. The forecast fitted to the model well. The findings derived from the study are to understand the nature and scale of possible rainfall variations in 28 stations of Bangladesh.

Acknowledgement

The authors would like to thank the Bangladesh Meteorological Department for providing support during this study.

References

Adamowski, J. and C. Karapataki (2010). Comparison of multivariate regression and artificial neural networks for peak urban water-demand forecasting: Evaluation of different ANN learning algorithms. *Journal of Hydrologic Engineering*, **15(10):** 729-743.

Afzal, M., Mansell, M.G. and A.S. Gagnon (2011). Trends and variability in daily precipitation in Scotland. *Procedia Environmental Sciences Journal*, **6(1):** 15-26.

Agrawal, A., Kumar, V., Pandey, A. and I. Khan (2012). An application of time series analysis for weather forecasting. *International Journal of Engineering Research and Applications*, **2(2),** 974-980.

Akhtar, M.K., Corzo, G.A., Andel, S.J.V. and A. Jonoski1 (2009). River flow forecasting with artificial neural networks using satellite observed precipitation pre-processed with flow length and travel time information: Case study of the Ganges river basin. *Hydrology and Earth System Sciences*, **13(9):** 1607-1618.

Alrumiah, R.M. and M.A. Fawzan (2002). Time series forecasting using wavelet denoising an application to Saudi stocks index. *Journal of King Saud University, Engineering Sciences*, **2(14):** 221-234.

Cannarozzo, M., Noto, L.V. and F. Viola (2006). Spatial distribution of rainfall trends in Sicily (1921–2000). *Physics and Chemistry of the Earth, Parts A/B/C*, **31(18):** 1201-1211.

Deo, R.C. and M. Sahin (2015). Application of the artificial neural network model for prediction of monthly standardized precipitation and evapotranspiration index using hydro meteorological parameters and climate indices in eastern Australia. *Atmospheric Research*, **161-162(1):** 65-81.

Dong, Z., Guo, X. and J. Zheng (2001). Calculation of noise resistance by use of the discrete wavelets transform. *Electrochemistry Communications*, **3(10):** 561-565.

Drápela, K. and I. Drápelová (2011). Application of Mann-Kendall test and the Sen's slope extimates for trend detection in deposition data from Bílý Kříž (Beskdydy Mts., the Czech Republic) 1997-2010. *Beskydy*, **4(2):** 133-146.

ESRI (2001). Using ArcGIS Geostatistical Analyst. The United States of America.

Hand, L.M. and J.M. Shepherd (2009). An investigation of warm-season spatial rainfall variability in Oklahoma

City: Possible linkages to urbanization and prevailing wind. *Journal of Applied Meteorology and Climatology*, **48(2):** 251-269.

Intergovernmental Panel on Climate Change (IPCC) (2007). Climate Change 2007: The Physical Science Basis. Contribution of Working Group I to the Fourth Assessment Report of the Intergovernmental Panel on Climate Change, edited by S. Solomon et al. Cambridge Univ. Press, New York.

KİSİ, Ő. (2003). Daily river flow forecasting using artificial neural networks and auto-regressive models. *Turkish Journal of Engineering and Environmental Sciences*, **29(1):** 9-20.

Khan, Y.A., Lateh, H., Baten, M.A. and A.A. Kamil (2011). Critical antecedent rainfall conditions for shallow landslides in Chittagong City of Bangladesh. *Environmental Earth Sciences*, **67(1):** 97-106.

Longobardi, A. and P. Villani (2009). Trend analysis of annual and seasonal rainfall time series in the Mediterranean area. *International Journal of Climatology*, **30(10):** 30-139.

Luís, M.D., Raventós, J., González-Hidalgo, J.C., Sánchez, J.R. and J. Cortina (2000). Spatial analysis of rainfall trends in the region of Valencia (East Spain). *International Journal of Climatology*, **20(12):** 1451-1469.

Marquínez, J., Lastra, J. and P. García (2003). Estimation models for precipitation in mountainous regions: The use of GIS and multivariate analysis. *Journal of Hydrology*, **270(1-2):** 1-11.

Miao, L., Jun, X. and M. Dejuan (2012). Long-term Trend Analysis of Seasonal Precipitation for Beijing, China. *Journal of Resources and Ecology*, **3(1):** 64-72.

Modarres, R. and A. Sarhadi (2009). Rainfall trends analysis of Iran in the last half of the twentieth century. *Journal of Geophysical Research*, **114(D3):** 1-9.

Nakhei, M. and S.A. Nasr (2012). A combined Wavelet-Artificial Neural Network model and its application to the prediction of groundwater level fluctuations. *Journal of Geopersia*, **2(2):** 77-91.

Nasri, M. and R. Modarres (2009). Dry spell trend analysis of Isfahan Province, Iran. *International Journal of Climatology*, **29(10):** 1430-1438.

Nejad, F.H. and V. Nourani (2012). Elevation of wavelet denoising performance via an ANN based stream flow forecasting model. *International Journal of Computer Science & Management*, **1(4):** 764-770.

Nury, A.H., Hasan, K. and M.J.B. Alam (2015). Comparative study of wavelet-ARIMA and wavelet-ANN models for temperature time series data in northeastern Bangladesh. *Journal of King Saud University-Science* (http://dx.doi.org/10.1016/j.jksus.2015.12.002).

Nury, A.H. and K. Hasan (2015). Analysis of drought in northwestern Bangladesh using standardized precipitation index and its relation to southern oscillation index. *Environmental Engineering Research*. Doi: http://dx.doi.org/10.4491/eer.2015.115.

Panigrahi, S., Karali, Y. and H.S. Behera (2013). Time series forecasting using evolutionary neural network. *International Journal of Computer Applications*, **75(10):** 13-17.

Partal, T. and E. Kahya (2005). Trend analysis in Turkish precipitation data. *Hydrological Processes*, **20(9):** 2011-2026.

Pinto, S.C., Adamowski, J. and G. Oron (2012). Forecasting urban water demand via wavelet-denoising and neural network models. *Water Resources Management*, **26(12):** 3539-3558.

Ramana, R.V., Krishna, B., Kumar, S.R. and N.G. Pandey (2013). Monthly rainfall prediction using wavelet neural network analysis. *Water Resource Management*, **27(10):** 3697-3711.

Ramazanipour, M. and M. Roshani (2011). Test and trend analysis of precipitation and discharge in the north of Iran. *World Applied Sciences Journal*, **14(9):** 1286-1290.

Salmi, T., M*äättää* , A., Anttila, P., Airola, T.R. and T. Amnell (2002). Detecting trends of annual values of atmospheric pollutants by the Mann-Kendall test and Sen's slope estimates – the Excel template application MAKESENS. Finnish Meteorological Institute, Helsinki. ISBN: 951-697-563-1.

Shahid, S. and O.S. Khairulmaini (2009). Spatio-temporal variability of rainfall over Bangladesh during the time period 1969-2003. *Asia-Pacific Journal of Atmospheric Sciences*, **45(3):** 375-389.

Shamsuddin, S. (2007). Spatial and temporal characteristics of droughts in the western part of Bangladesh. *Hydrological Processes*, **22(13):** 2235-2247.

Shamsuddin, S. (2011). Trends in extreme rainfall events of Bangladesh. *Theoretical and Applied Climatology*, **104(3):** 489-499.

Stern, N. (2007). Report of the Stern Review: The Economics of Climate Change. HM Treasury, London. ISBN: 9780521700801.

Wadi, A.S., Ismail, T.M., Alkhahazaleh, H.M. and A.S. Karim (2011). Selecting wavelet transforms model in forecasting financial time series data based on ARIMA model. *Applied Mathematical Sciences*, **5(7):** 315-326.

Yu, I.K., Kim, C.I. and Y.H. Song (2000). A novel short-term load forecasting technique using wavelet transform analysis. *Electric Power Systems Research-Journal*, **28(6):** 537-549.

Yue, S., Pilon, P. and G. Cavadias (2002). Power of the Mann-Kendall and Spearman's rho tests for detecting monotonic trends in hydrological series. *Journal of Hydrology*, **259(1-4):** 254-271.

Yue, S. and C. Wang (2004). The Mann-Kendall Test Modified by Effective Sample Size to Detect Trend in Serially Correlated Hydrological Series. *Water Resources Management*, **18(3):** 201-218.

Asian Journal of Water, Environment and Pollution

Volume 13 Number 1 **January – March, 2016**

Contents